PNAS RESEARCH ARTICLE | GENETICS

Multivariate genetic architecture reveals testosterone-driven sexual antagonism in contemporary humans

Anasuya Chakrabarty[a,1], Saikat Chakraborty[a,b], Diptarup Nandi[a,c], and Analabha Basu[a,1]

Edited by Marcus Feldman, Stanford University, Stanford, CA; received March 1, 2024; accepted May 6, 2024

Sex difference (SD) is ubiquitous in humans despite shared genetic architecture (SGA) between the sexes. A univariate approach, i.e., studying SD in single traits by estimating genetic correlation, does not provide a complete biological overview, because traits are not independent and are genetically correlated. The multivariate genetic architecture between the sexes can be summarized by estimating the additive genetic (co)variance across shared traits, which, apart from the cross-trait and cross-sex covariances, also includes the cross-sex-cross-trait covariances, e.g., between height in males and weight in females. Using such a multivariate approach, we investigated SD in the genetic architecture of 12 anthropometric, fat depositional, and sex-hormonal phenotypes. We uncovered sexual antagonism (SA) in the cross-sex-cross-trait covariances in humans, most prominently between testosterone and the anthropometric traits – a trend similar to phenotypic correlations. 27% of such cross-sex-cross-trait covariances were of opposite sign, contributing to asymmetry in the SGA. Intriguingly, using multivariate evolutionary simulations, we observed that the SGA acts as a genetic constraint to the evolution of SD in humans only when selection is sexually antagonistic and not concordant. Remarkably, we found that the lifetime reproductive success in both the sexes shows a positive genetic correlation with anthropometric traits, but not with testosterone. Moreover, we demonstrated that genetic variance is depleted along multivariate trait combinations in both the sexes but in different directions, suggesting absolute genetic constraint to evolution. Our results indicate that testosterone drives SA in contemporary humans and emphasize the necessity and significance of using a multivariate framework in studying SD.

sex difference | genetic correlations | additive genetic (co)variance matrix | human complex traits | **B** matrix

Significance

Sex difference (SD) is widespread in humans, though they share the same genome. Single traits are generally studied to explore such differences in humans. But traits do not occur in isolation and share a common genetic basis. We investigated the genetic architecture of anthropometric, fat depositional, and sex-hormonal phenotypes, and found that sexes are not only dissimilar, but the same set of alleles act in opposite directions in the sexes, especially between testosterone and the anthropometric traits. Importantly, the shared genetic architecture between the sexes constrains the evolution of SD only when selection is sexually divergent. This work uncovers the role of testosterone in regulating SD and extends our understanding of SD in contemporary humans beyond what isolated traits reveal.

Sex difference (SD) is widespread among complex traits and disorders in humans (1–6), even though males and females share almost their entire genomes. Moreover, the genes on the autosomes occur half of the time in either males or females. Despite the ubiquity, the evolution of SD is nontrivial. When sexual/natural selection shifts one of the sexes from a common phenotypic optimum, the shared genetic architecture often leads to genetic constraint to independent evolution of the sexes (7). Sex-specific selection leads to intralocus sexual conflict (IASC) where one or both the sexes are displaced from their phenotypic optima (8). The strength of the cross-sex genetic correlation (r_{mf}), i.e., the genetic correlation of a shared homologous trait between the sexes, is a good approximation of the extent of IASC and the degree of sexual dimorphism (9). If males and females have the same genetic architecture for a shared trait then the r_{mf} is expected to be 1. This is because, if the strength of the cross-sex genetic correlation is high for a trait, then selection on one sex would lead to a strong correlated response in the other sex, generally intensifying IASC. Though at times, traits which are phenotypically dimorphic can exhibit high r_{mf} which indicates little genetic variation is left for the evolution of dimorphism (8). But, generally for a shared trait, sexual dimorphism finally evolves when the r_{mf} is eroded under persistent sex-specific selection and IASC is fully or partially resolved through mechanisms like sex-biased gene expression, genomic imprinting, etc. (8–11).

On the other hand, most often traits do not occur in isolation, but in functionally related modules due to pleiotropy and/or linkage disequilibrium. Hence, when we investigate SD, estimating a univariate measure like r_{mf} for one shared trait is not adequate to understand the genetic basis of SD. The interdependence of traits and their multivariate genetic architecture can be statistically summarized using the additive genetic variance–covariance matrix, **G** (12), which is a square and symmetric matrix containing the additive genetic variances of traits in the diagonal and the additive genetic covariances between traits in the off diagonals. Under a multivariate framework, $\mathbf{G}_{\mathrm{mf}}$ for shared traits between males and females can be partitioned into four submatrices (7):

Author contributions: A.C., S.C., and A.B. developed the theory for prediction of cross-sex-cross-trait genetic correlations; A.C. and S.C. designed research; A.C. performed research; A.B. contributed new reagents/analytic tools; A.C. and D.N. analyzed data; and A.C., S.C., D.N., and A.B. wrote the paper.

Competing interest statement: S.C. is currently an employee of GSK. The work included in this manuscript was performed when S.C. was working at the Biotechnology Research Innovation Council- National Institute of Biomedical Genomics, Kalyani. All views and opinions expressed in this manuscript are solely of the authors' and do not in any manner reflect the official stand of GSK.

This article is a PNAS Direct Submission.

[1]To whom correspondence may be addressed. Email: ac4@nibmg.ac.in or ab1@nibmg.ac.in.

This article contains supporting information online at https://www.pnas.org/lookup/suppl/doi:10.1073/pnas.2404364121/-/DCSupplemental.

Published June 4, 2024.

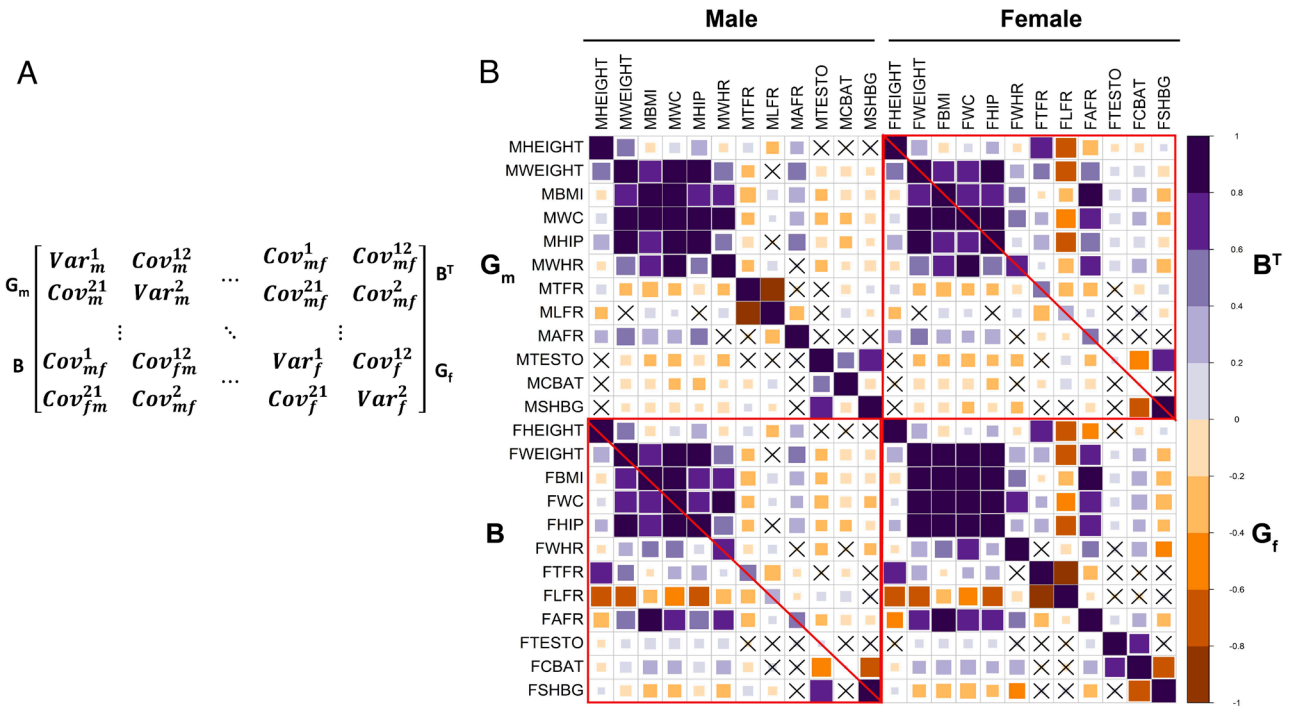

Fig. 1. $\mathbf{G}_{mf}$ matrix in males and females. (*A*) Schematic showing $\mathbf{G}_{mf}$ genetic covariance matrix and its constituents $\mathbf{G}_m$, $\mathbf{G}_f$, **B**, and $\mathbf{B}^T$ for two traits in males and females. (*B*) $\mathbf{G}_{mf}$ correlation matrix for all the 12 traits in both the sexes. The male cross-trait genetic correlations ($\boldsymbol{G_m/r_{ctM}}$) are on the top left and female cross-trait genetic correlations ($\boldsymbol{G_f/r_{ctF}}$) are on the bottom right. The cross-sex genetic correlations ($\boldsymbol{r_{mf}}$) are along the red diagonals of the top right and bottom left squares of the **B** and $\mathbf{B}^T$ matrix. The off-diagonal genetic correlations in the **B** and $\mathbf{B}^T$ (red squares) are the cross-sex-cross-trait genetic correlations ($\boldsymbol{r_{mf}^{ct}}$). Genetic correlations which are not significantly different from zero are marked with crosses, except the diagonal of the **B** and $\mathbf{B}^T$ which are tested for significantly different from 1. The size of the yellow and purple squares is according to the strength of the correlations.

$$\mathbf{G_{mf}} = \begin{bmatrix} \mathbf{G_m} & \mathbf{B} \\ \mathbf{B^T} & \mathbf{G_f} \end{bmatrix}, \qquad [1]$$

where $\mathbf{G}_m$ and $\mathbf{G}_f$ are the male and female within-sex **G** matrices, **B** is the cross-sex genetic covariance matrix and $\mathbf{B}^T$ is the transpose of **B**. **B** consists of cross-sex genetic covariances in the diagonal and cross-sex-cross-trait genetic covariances in the off-diagonals (Fig. 1*A*). For traits i and j, there could be two measures of cross-sex-cross-trait covariances, (or cross-sex-cross-trait genetic correlations, r_{mf}^{ct}) i.e., $\mathrm{Cov}(\mathrm{Trait i}_f, \mathrm{Trait j}_m)$ and $\mathrm{Cov}(\mathrm{Trait i}_m, \mathrm{Trait j}_f)$, e.g., genetic correlation between height in females and weight in males, and height in males and weight in females. Unlike **G**, **B** might not always be symmetrical, i.e., $\mathbf{B} \neq \mathbf{B}^T$, as these covariances might differ depending on the trait expressed in a specific sex. Hence, the additive effects of the alleles on shared traits differ based on the sex where the traits are expressed. The evolution of sexual dimorphism causes the within-sex **G** to diverge and induces asymmetry in **B** (13, 14) which signifies difference in the multivariate genetic architecture of the sexes. Exploring SD solely based on r_{mf} might lead to erroneous conclusions as even if r_{mf} is high, which translates to low levels of dimorphism, low r_{mf}^{ct} can still facilitate the evolution of SD (14). Hence, **B** can hinder or facilitate evolution of sexual dimorphism and can elicit completely different directions of evolutionary response in males and females even to sexually concordant selection (14, 15).

Sexually antagonistic (SA) genetic variation, where alleles beneficial to one sex are harmful to the other, can arise due to SA selection, signatures of which are found on the human genome (16). Opposing signs of cross-sex genetic covariance in the off-diagonal elements of **B** can imply SA genetic variation if traits are associated with fitness. When IASC is acute, i.e., there is strong SA selection with SA allelic effects on fitness, the r_{mf} of fitness is generally negative, and it only goes back to 1 when IASC is fully resolved. Hence, a r_{mf} of fitness less than 1 suggests only partially resolved IASC. Difference in signs of the off diagonals of **B** (cross-sex-cross-trait genetic covariances) can also contribute to the asymmetry in **B** irrespective of their association with fitness. Asymmetry in **B** in turn reflects SD in the genetic architecture of complex traits, which can be unequivocally captured only under a multivariate framework. **B** can change the direction of an otherwise divergent evolutionary response to SA selection and can constrain the sexes to evolve in similar directions (17).

Phenotypically, anthropometric traits such as height and fat depositional traits like trunk and arm fat show SD in humans. Traits like BMI and waist to hip ratio (WHR) are influenced by differential fat deposition in different parts of the body, and such fat deposition patterns are known to differ between the sexes (18–20). Moreover, fat deposition is also regulated by sex hormones (19) via androgen receptors present in the adipose tissue (21). In fact, one of the major differences between males and females is the difference in circulating levels of sex hormones, such as testosterone. Along with genetic pleiotropy, hormones can also influence many traits at a time, leading to hormonal pleiotropy, and can directly influence genetic covariances (22, 23), which can have evolutionary implications. For example, it has been shown that experimental treatment with testosterone can change the genetic architecture of morphological traits in female *Anolis* lizards, making them indistinguishable from that of the male (22). Testosterone can differentially affect males and females at the phenotypic level which can stem from differences in pleiotropy (genetic) between testosterone and other traits in the two sexes. We conjecture that SDs in humans can be largely modulated by differential influence of sex hormones on other groups of traits, e.g., anthropometric, and fat depositional. However, such studies

investigating the role of hormonal pleiotropy in the maintenance of sex-specific genetic architecture in humans are largely missing.

Contemporary human genetics is largely dominated by genome-wide association studies (GWAS) where sex is mostly treated as a factor and is controlled for in the statistical model, which adjusts for any sex-specific variation in the data. Two broad categories of studies explore SDs in genetic architecture in humans—a) sex-stratified GWAS which attempts to find sex-specific SNPs, effect sizes, or allelic directions (24–30), and b) estimating r_{mf} and/or sex-specific heritabilities using individual-level genetic data (2, 3, 5, 31–34) or GWAS summary statistics (25, 32, 35–39). Though there has been a surge of sophisticated methods for estimating genetic correlations using (i) individual-level genetic data and (ii) GWAS summary statistics, indirect effects of cross-trait covariances across sexes (off diagonals of **B**) on SD have not been estimated. But in nonhuman species, **B** is routinely studied and are essential in exploring the evolution of SD (13, 14, 17, 40, 41).

In this study, we investigated SDs in the within and across-sex genetic architecture of three trait categories, i.e., a) anthropometric (six traits), b) fat depositional (three traits), and c) sex-hormonal (three traits), at different levels:

i) We estimated the entire $\mathbf{G}_{\text{mf}}$ (co)variance matrix along with the cross-trait (r_{ct}), cross-sex (r_{mf}), and cross-sex-cross-trait (r^{ct}_{mf}) genetic correlations for 12 traits in each sex from GWAS summary statistics as a measure of SD, and to assess the degree of hormonal pleiotropy between sex hormones and other traits.

ii) We evaluated whether the between-sex genetic covariance matrix, **B,** acts a constraint to the evolution of SD in these traits in humans in the face of simulated sexually concordant and antagonistic selection, and ascertained the degree of asymmetry in **B**.

iii) We estimated the genetic correlation (r_{ct}) between lifetime reproductive success (LRS) in humans and the 12 traits in males and females to find their association with fitness. We also estimated the r_{mf} of LRS to detect the degree of IASC in humans.

iv) We inspected the degree of polygenic overlap between traits in males and females to estimate the number of shared variants using bivariate Gaussian mixture models.

v) Finally, we identified the genome-wide significant variants shared between the traits in both the sexes, annotated them, and tested for enrichment in biological pathways to explore sex-specificity. Additionally, we performed colocalization to examine pleiotropy between testosterone and BMI in males and females.

Results

Traits and GWAS Summary Statistics. We used publicly available GWAS summary statistics from published studies and databases to estimate genetic correlations. All the summary statistics are from sex-stratified GWAS, performed on UK Biobank data. The anthropometric traits include height, weight, BMI, waist circumference (WC), hip circumference (HIP), and waist-to-hip ratio (WHR). Arm fat ratio (AFR), leg fat ratio (LFR), and trunk fat ratio (TFR) are the fat depositional traits. The sex-hormonal traits are total testosterone (TESTO), calculated bioavailable testosterone (CBAT), and sex hormone–binding globulin (SHBG).

All the traits were normalized before performing GWAS. The anthropometric traits were inverse-rank normal transformed, and the fat ratios were rank transformed. The sex hormones were normalized using log-transformation. Consequently, the genetic covariances as well as the correlations were not affected by any heterogeneity in trait distributions.

We also estimated the phenotypic correlation between 11 of the 12 traits (except CBAT) from 203,146 males and 241,041 females from individual-level data from UK Biobank (42). The direction of the phenotypic correlations closely mirrors that of the genetic correlations indicating genetic and environmental correlations have the same directions (Dataset S15).

We estimated the additive genetic variances and covariances (elements of $\mathbf{G}_{\text{mf}}$) and the r_{ct}, r_{mf}, and r^{ct}_{mf} using the LD score regression (LDSC) framework (43) (Fig. 1, and Datasets S1–S4 and S9).

Cross-Trait Genetic Correlations (r_{ct}). The r_{ct} are the genetic correlations between traits within each sex (Figs. 1 and 2 *A* and *B* and *SI Appendix*, Figs. S1–S3). All the r_{ct} are moderate to high, and the three trait categories, i.e., anthropometric, fat depositional, and sex-hormonal, show SDs for r_{ct} with nonoverlapping 95% CI (Fig. 2 *A* and *B*). Overall, the fat depositional traits, and testosterone and CBAT among the hormonal traits, show most of the differences in r_{ct}. Out of 66 r_{ct} in males and females, 32 and 27 genetic correlations were negative, respectively (Datasets S1 and S2).

Anthropometric and Fat Depositional Traits. Among the anthropometric traits, r_{ct} are significantly different between the sexes for 9 traits including height and weight (*SI Appendix*, Fig. S1). r_{ct} of fat ratios show SD except between TFR and LFR (*SI Appendix*, Fig. S2). r_{ct} between TFR and LFR are strongly negative in both males and females (−0.92 ± 0.005, −0.91 ± 0.004), similar to that observed by Rask-Andersen et al. (25). r_{ct} of fat ratios with other traits show sex-specific trends, with r_{ct} between TFR and other anthropometric traits being negative in males, whereas between LFR and anthropometric traits being negative in females (*SI Appendix*, Fig. S2). r_{ct} between AFR and the anthropometric traits are positive in both males and females except with height, which is moderately negative in females (−0.40 ± 0.02), but positive in males (0.26 ± 0.02). AFR and BMI show very strong positive correlation (r_{ct}) in females (0.94 ± 0.004), and moderately high in males (0.39 ± 0.02), but the r_{ct} between LFR and BMI is negative in females (−0.33 ± 0.02) and positive in males (0.17 ± 0.02). This indicates that the variants which are involved in increasing BMI decrease LFR but increase AFR in females. Hence, females with high BMI stores fat mostly in arms and not in legs.

Sex-Hormonal Traits. Both testosterone and CBAT show clear sex-specific trends in the r_{ct} with anthropometric traits, positive in females but negative in males (Fig. 2 *A* and *B*). CBAT-anthropometric traits r_{ct} is higher in females, compared to testosterone-anthropometric traits. CBAT-WC r_{ct} is the highest (0.37 ± 0.03) in females whereas testosterone-WC r_{ct} is highest (−0.25 ± 0.04) in males. The SHBG-anthropometric traits r_{ct} are all negative in both the sexes, whereas between SHBG and AFR is negative in females (*SI Appendix*, Fig. S3). SHBG shows no significant r_{ct} with the other fat depositional traits. With testosterone, the r_{ct} of SHBG is strongly positive (0.79 ± 0.03), whereas with CBAT is small but negative (−0.17 ± 0.04). The fat ratios show no significant r_{ct} with TESTO or CBAT in either sex, except for AFR-TESTO r_{ct} in females, which is moderately positive and significant (0.29 ± 0.03). Testosterone

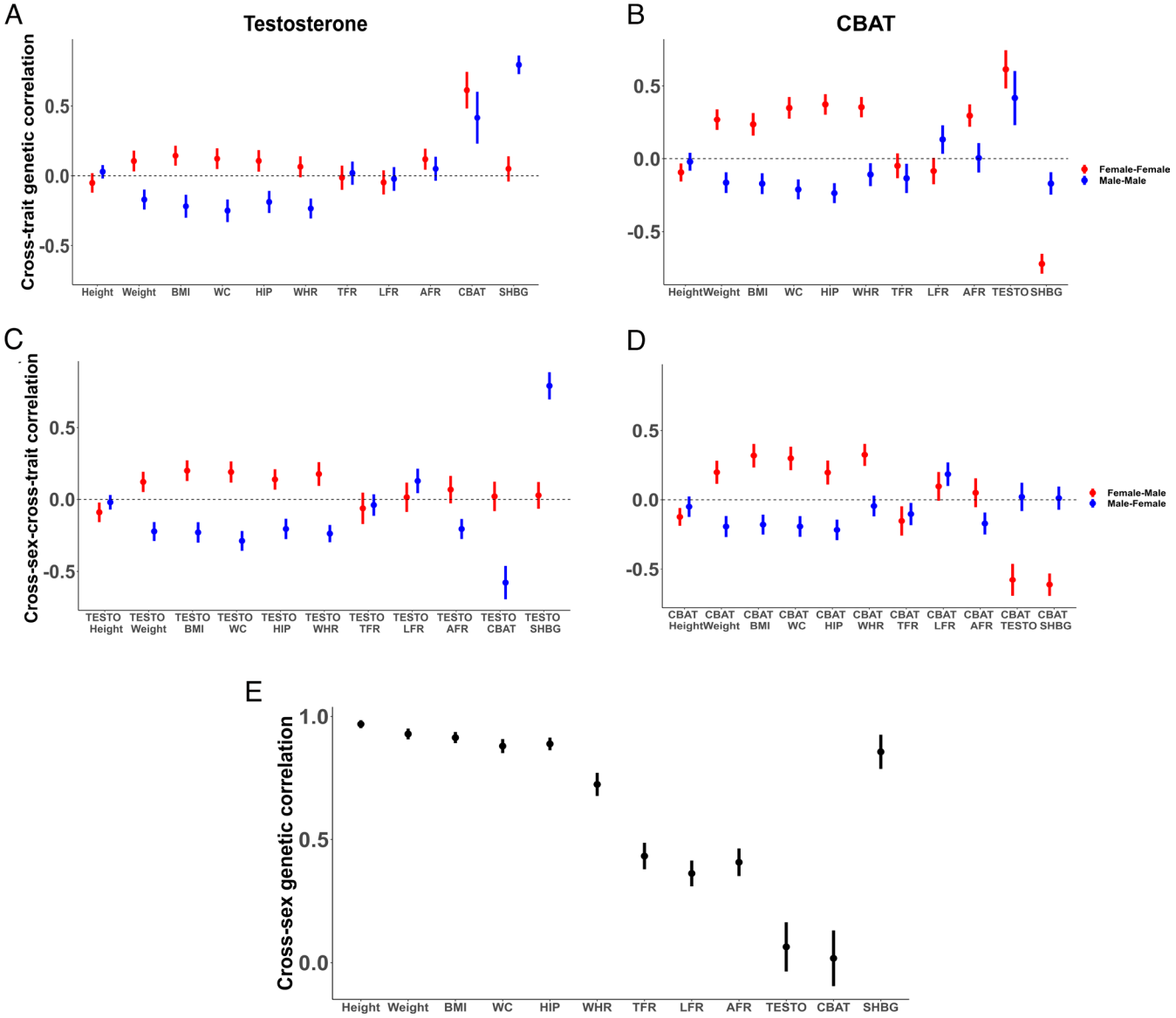

Fig. 2. Genetic correlations of all 12 traits with testosterone and CBAT. (*A* and *B*) cross-trait genetic correlations of testosterone and CBAT with anthropometric and fat depositional traits in males and females (r_{ct}), respectively. (*C* and *D*) Cross-sex-cross-trait genetic correlations of testosterone and CBAT with other traits (r_{mf}^{ct}). (*E*) Cross-sex genetic correlations (r_{mf}) of all 12 traits.

showed positive phenotypic correlation with anthropometric traits in females but negative in males.

Cross-Sex Genetic Correlations (r_{mf}). The cross-sex genetic correlation r_{mf} denotes the degree of genetic basis of sexual dimorphism for *a* trait. The r_{mf} are the correlations between the same homologous trait in males and females (Figs. 1 and 2*E*). r_{mf} is highest for height (0.96 ± 0.008), and lowest for CBAT (0.01 ± 0.05) (Dataset S3). Other than CBAT and testosterone, the most dimorphic trait is LFR, with a r_{mf} of 0.36 ± 0.02. The null expectation is r_{mf} =1 when there is no difference in the genetic architecture between the sexes for the same traits. We found that all the r_{mf} were significantly different from 1 (Dataset S3), which is expected given the high sample size in the UK Biobank. The anthropometric traits have the highest r_{mf} and therefore are the least dimorphic, and the fat ratios lie in between the anthropometric traits and testosterone.

Cross-Sex-Cross-Trait Genetic Correlations (r_{mf}^{ct}). The r_{mf}^{ct} are the correlations between trait *A* expressed in males and trait *B* expressed in females and vice versa (Fig. 1*B*). Out of 66 pairs of r_{mf}^{ct}, 18 pairs of statistically significant correlations were of opposite signs (Dataset S4), suggesting the presence of sexual antagonism (SA). We would expect that the r_{mf}^{ct} would be equal, i.e., the off-diagonal elements of **B** would be equal (symmetric). Hence, the null expectation is of no antagonism (i.e., equal correlations with the same sign). We estimated the bootstrap CI of the number of opposing correlations and did not find an overlap with zero (CI = 16 to 25). Most of the male–female and female–male genetic correlations were significantly different from each other, except for SHBG (*SI Appendix*, Fig. S6). Among the r_{mf}^{ct} with opposite signs were also the correlations between testosterone-anthropometric, and CBAT-anthropometric traits (Fig. 2 *C* and *D* and *SI Appendix*, Figs. S5 and S6). Hence, variants increasing testosterone in females also increase BMI in males (0.20 ± 0.03), but variants which increase testosterone in males decrease BMI in females (−0.23 ± 0.04) (as the direction of genetic correlation is the opposite in the two cases). Similar difference in r_{mf}^{ct} was found between LFR and BMI in males and females. We have observed that the signs for r_{ct} in males and females resemble that of r_{mf}^{ct} for most of the traits. For e.g., the r_{ct} between testosterone-BMI is positive in females but

negative in males, which matches the sign of the r_{mf}^{ct} between the two traits. Such opposing influence of testosterone is also evident in the phenotypic correlations (Dataset S15). This observed SA in the cross-sex-cross-trait genetic correlations is mostly driven by testosterone.

We found that $\boldsymbol{B} \neq \boldsymbol{B}^{\boldsymbol{T}}$, i.e., the off diagonals of **B** (r_{mf}^{ct}) are not equal. Asymmetry in **B** is the manifestation of underlying difference in genetic architecture of the sexes. We have decomposed **B** into its symmetric and skew-symmetric components, and by partitioning the sum of squares (SS) of **B**, have quantified the proportion of SS in **B** which is skew-symmetric as a measure of asymmetry. We found that 14.4% of **B** is skew-symmetric (Dataset S8), which is high given that the null expectation is of complete symmetry (i.e., 0% asymmetry). This extent of asymmetry in the cross-sex covariance matrix **B** demonstrates the differences in the multivariate genetic architecture of the sexes.

We dropped the sex-hormonal traits (TESTO, CBAT, SHBG) from **B**, and re-estimated asymmetry, and the percentage of skew symmetry decreased to 11.5%. When only the anthropometric traits were included in the analysis, the asymmetry dropped to 1%. Moreover, when only fat ratios and sex-hormonal traits were analyzed, the asymmetry of **B** increased to 24.2%. Thus, most of the asymmetry in **B** is contributed by the fat depositional and sex-hormonal traits.

The differences between pairs of r_{mf}^{ct} are contributed both by differences in the cross-sex-cross-trait genetic covariances (off diagonals of **B**) as well as the differences in genetic variance between the sexes (see Eq. **5** in *Materials and Methods*). For the anthropometric traits there was no difference in the genetic variance (heritabilities) between males and females (*SI Appendix*, Fig. S9). However, for the fat ratios and testosterone, the genetic variances show sex-specific differences. Hence, the differences in the r_{mf}^{ct} involving testosterone and the fat ratios are contributed by both their sex-specific heritabilities as well as the differences in cross-sex-cross-trait genetic covariances. We found that the r_{mf}^{ct} can be predicted from the product of the cross-sex and cross-trait genetic correlations only if the $r_{ct} \approx 1$ or the $r_{mf} \approx 1$ (*SI Appendix*, Supplementary Note).

Genetic Correlation with Fitness. To explore how the traits in our study correlate with fitness, we estimated the r_{ct} between LRS and the traits in males and females separately. We found a significant positive genetic correlation between LRS and weight, WC, HIP, BMI, and WHR in both males and females, and these correlations were significantly different between the sexes except for WHR (Dataset S10 and *SI Appendix*, Fig. S10). Some of these genetic correlations between relative-LRS (rLRS) and the anthropometric traits were previously reported by Sanjak et al. (44). Height was negatively correlated with LRS but only in females. Among the fat ratios, arm fat in females and leg fat in males showed positive genetic correlations. Interestingly, trunk fat was negatively correlated with LRS in both the sexes. For these two traits, height and TFR, which showed negative correlations, we also measured the r_{mf}^{ct} with LRS. We found a negative genetic correlation of female LRS with male TFR and height, indicating SA in fitness in humans. SHBG was the only sex hormone which showed negative correlation in males, but apart from that none of the hormonal traits were found to be significantly correlated with LRS in both males and females.

Theory predicts that when SD evolves, the r_{mf} of fitness (r_{mf}^{W}) becomes strongly negative under SA selection, and IASC is acute. As sexes reach their sex-specific phenotypic optima, the r_{mf}^{W} goes back to 1 when IASC is fully resolved. Hence, a r_{mf}^{W} less than 1 signifies partially resolved IASC. To examine the degree of IASC in humans, we estimated the r_{mf}^{W} of LRS and found it to be significantly less than 1 ($r_{mf}^{W} = 0.61$, $P = 8.72 \times 10^{-14}$). A positive r_{mf}^{W} can also signify unresolved SA selection and hence IASC, as the theoretical prediction of a negative r_{mf}^{W} is often conservative evidence of SA (45).

Matrix Comparison and Genetic Constraint. To investigate SD in the multivariate genetic architecture of the traits considered, we compared $\mathbf{G}_m$ and $\mathbf{G}_f$, both including and excluding **B**. We found that the entire $\mathbf{G}_{mf}$ as well as $\mathbf{G}_m$ and $\mathbf{G}_f$ were not full rank matrices, i.e., some of the eigenvalues were zero for the corresponding eigenvectors. On eigendecomposition, $\mathbf{G}_m$, $\mathbf{G}_f$, and $\mathbf{G}_{mf}$ have 2 out of 12, 1 out of 12, and 5 out of 24 negative eigenvalues, respectively (Datasets S11–S13), which indicates the eigenvalues are essentially zero and due to floating point error are denoted as negative. Biologically, this means that there is no genetic variance for certain linear combinations of the traits in the phenotypic space which makes the **G** matrices singular. We checked the determinants of all the three matrices, and they were all zero, corroborating the singularity of these matrices. **G** matrices are often singular which represents absolute multivariate constraint to evolution due to absence of genetic variance in certain directions (46, 47). When we did an eigendecomposition of the phenotypic correlation matrices (**P**), they were both singular in males and females (Dataset S16). The corresponding two eigenvectors in males ($\mathbf{G}_m$) with zero eigenvalues showed maximum loading for WC and TFR, respectively, and in females for only WC (Datasets S12 and S13). This represents an absolute genetic constraint along those directions in the multivariate trait space if selection acts along those directions. This happens as there are traits which are exact linear combinations of WC and TFR in our **P** and **G**s. When we dropped these traits from $\mathbf{G}_m$ and $\mathbf{P}_m$, and only WC from $\mathbf{G}_f$ and $\mathbf{P}_f$, the eigenvalues were small but no longer zero, and hence the matrices were full rank. But as we were interested in the genetic architecture of correlated traits, we kept these traits in our analyses. We found that the effective number of dimensions for $\mathbf{G}_m$ and $\mathbf{G}_f$ are only 2.45 and 2.25, respectively (*SI Appendix*). The first two eigenvectors for $\mathbf{G}_m$ explain 62% of the genetic variance while that of $\mathbf{G}_f$ explains 75% of the genetic variance. Hence, more than half of the genetic variance is described by the first two eigenvectors in males and females, which explains the effective dimensionality of the **G** matrices. This signifies that the sizes of the eigenvalues of both the matrices have a very uneven distribution indicating ill-conditioned **G** matrices.

To compare $\mathbf{G}_m$ and $\mathbf{G}_f$ we used the random skewers method (48) which is based on Lande's multivariate breeder's equation (12), $\boldsymbol{\Delta z = G\beta}$, where $\Delta\mathbf{z}$ is the short-term evolutionary response to selection, **G** is the **G** matrix and β is the selection gradient (*SI Appendix*). If we multiply two **G** matrices with the same selection vectors, any difference in the evolutionary response would be due to the difference in **G**s, which is the basic principle of the random-skewers method. To tease apart the effect of **B**, we measured the response to selection in both the sexes with **B** and then again by constraining **B** to zero (*SI Appendix*, **Eq. S2**). We used 1,000 random skewers (random selection vectors) under sexually concordant as well as antagonistic selection pressure. We measured the vector correlation between the predicted response in males and females ($\Delta\mathbf{z}_m$ and $\Delta\mathbf{z}_f$), which is the cosine of the angle between the two vectors, to compare $\mathbf{G}_m$ and $\mathbf{G}_f$. The null expectation is a correlation of 1, i.e., when there is no difference in genetic architecture between the sexes. We found that the median [95% CI] vector correlation without **B** is 0.81 [0.75–0.94] and with **B** is 0.84 [0.30–0.92] which are high but significantly

different from 1, indicating that the multivariate genetic architecture of sexes differs from each other.

Using these same angles between male and female responses, we also investigated how **B,** i.e., the shared genetic architecture between the sexes acts as a genetic constraint to the evolution of SD. Here, an angle (θ) > 0° between the male and female responses indicated that sexes can evolve in different directions. We observed that under concordant selection (selection vectors in the same direction), the angle between male and female response vectors were moderate both without **B** (median θ with 95% CI) between $\Delta\mathbf{z}_m$ and $\Delta\mathbf{z}_f$ = 35.67 ° [20°–41.61°] and with **B** (θ between $\Delta\mathbf{z}_{mB}$ and $\Delta\mathbf{z}_{fB}$ = 30.74° [21.83°–73.97°]) (Fig. 3*A*). Due to the overlap of these two angles, **B** does not constrain or facilitate the independent evolution of sexes in humans when selection is sexually concordant.

When we projected random selection vectors in opposing directions (antagonistic) through the $\mathbf{G}_{mf}$ constraining **B** to zero, we found that the median angle between $\Delta\mathbf{z}_m$ and $\Delta\mathbf{z}_f$ was extremely large (Fig. 3*B*), 145.2° [135.4°–158.4°], which means the sexes can evolve independently in different directions in response to antagonistic selection. But when we included **B**, the angle between $\Delta\mathbf{z}_{mB}$ and $\Delta\mathbf{z}_{fB}$ drastically decreased by 72% to 58.3° [51.5°– 98.5°]. Hence, **B** acts as a constraint to the evolution of SDs when selection is sexually antagonistic by decreasing the angle between male and female predicted responses, compelling them to evolve in similar directions. But this angle between $\Delta\mathbf{z}_{mB}$ and $\Delta\mathbf{z}_{fB}$ overlapped between antagonistic (58.3° [51.5°–98.5°]) and concordant (30.74° [21.83°–73.97°]) selections. Hence, SD would evolve to a similar degree both under sexually concordant and antagonistic selection.

Genetic Overlap and Polygenicity. We have estimated the number of variants affecting each trait independently as well as those influencing combinations of traits (Fig. 4), by implementing bivariate Gaussian mixture models using *MIXeR* (49) (*SI Appendix*). Among the 24 traits, we found that the most polygenic with the largest number of causal variants is male WHR (Mean ± SE, 11.2K ± 1.2K), whereas the least polygenic is male SHBG (0.40K ± 0.07K). These causal variants explain 90% of SNP heritability of these specific traits. In case of the overlap between testosterone, and weight, BMI, WC, and HIP in males, all the variants which affect testosterone also influence the other traits (Fig. 4*A*). But in females, testosterone has unique causal variants besides having overlapping variants (80%) with weight, BMI, WC, and HIP. Moreover, the fraction of concordant variants (same direction of effect sizes) between testosterone and these four traits in males are between 10% and 26%, but much higher, between 60% and 74%, in females. 52.8% of the shared variants between male and female testosterone are concordant which signifies that equal number of shared variants have opposite effect sizes which renders the genetic correlation between the two traits not significantly different from zero. Polygenic overlap is also estimated between the fat ratios and the anthropometric traits, which show sex-specific differences (Fig. 4 *B* and *C* and *SI Appendix*, Fig. S7). The estimated number of causal variants in MIXeR depends on the sample size of the original GWAS. With the increase in sample size, the power to estimate causal variants of a trait increases.

Overlapping SNPs and Colocalization. We classified genome-wide variants into three broad categories based on their *P* values, separately for males and females. For this classification, we identified all the SNPs below the genome-wide significance at $\alpha = 5 \times 10^{-8}$, 1) that are shared between a pair of traits, 2) significant only in trait1, and 3) significant only in trait2. Fig. 5*A* shows the genome-wide distribution of these three SNP classes for testosterone and BMI in males and females (see *SI Appendix*, Fig. S9 for similar shared SNPs between AFR, TFR, and LFR, and BMI). We have observed that there are no shared SNPs which are significant for both testosterone and BMI in females, but we have found 38 significant shared SNPs in males. We identified five shared causal variants which show pleiotropic signals for testosterone and BMI in males with a PPH4 ≥ 0.9 in chromosome 16 (Dataset S14) through colocalization. We plotted some of these pleiotropic variants between testosterone and BMI in chromosome 16 for male and female testosterone using LocusZoom plots (Fig. 5*B*)

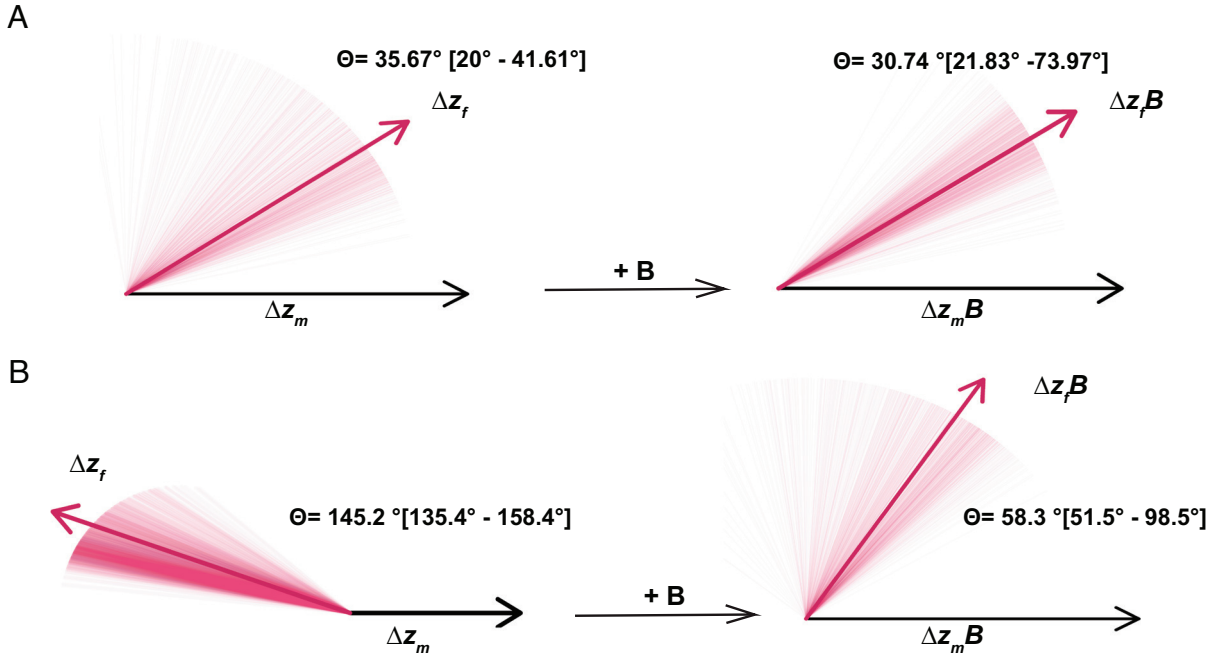

Fig. 3. Random selection skewers and genetic constraint to the evolution of sexual dimorphism. (*A*) Angle between the predicted responses to concordant selection vectors ($\Delta\mathbf{z}_m$ and $\Delta\mathbf{z}_f$) in males and females, respectively, constraining **B** to be zero, and after the inclusion of **B** ($\Delta\mathbf{z}_{mB}$ and $\Delta\mathbf{z}_{fB}$). The thin lines depict 1,000 response vectors, and the thick arrow is the median response. (*B*) Similar angles between male and female predicted responses before and after inclusion of **B**, but to antagonistic selection vectors. Here, **B** constrains the male and female evolutionary response vectors to evolve close to each other by reducing the angle between them. The length of the vectors is just for representation purpose.

to show that the same variants which are pleiotropic between testosterone and BMI in males are way below the significance threshold for female testosterone. The plots were zoomed around the SULT1A1 gene which we identified to be expressed in both testis and adipose tissue (*SI Appendix*). In chromosome 3, we detected colocalization of 3 more causal variants in males with a PPH4 = 1 (Dataset S14). Though we detected shared significant variants for testosterone and BMI in chromosome 2, we could not identify shared causal variants associated with both traits using colocalization, but we found independent causal variants (H_3). For females, we could not detect any colocalization signals in any of the three chromosomes between testosterone and BMI.

Discussion

In this study, we showed that there is sex difference (SD) in the multivariate genetic architecture of human anthropometric, fat depositional, and sex-hormonal phenotypes. We observed a plethora of cross-sex genetic covariances across traits with opposing directions mostly with testosterone, which was also reflected in the phenotypic correlations. This implies that testosterone drives sexual antagonism (SA) in the anthropometric traits both at the genetic and phenotypic levels. We also found that the shared genetic architecture between the sexes acts as a genetic constraint to the evolution of SD only when selection is sexually antagonistic and not concordant. We demonstrated that LRS in humans is positively correlated with anthropometric traits except height, but not with testosterone. Finally, we found additive genetic variance to be depleted in the multivariate phenotypic space along different directions in males and females, creating an absolute genetic constraint to evolution in those directions, possibly because of natural or sexual selection.

We found extensive evidence for SA in our study, notably between the sex-hormonal phenotypes (testosterone and CBAT) and the anthropometric traits. Here, we have shown the existence of multivariate SA as evident from 27% of the r_{mf}^{ct}, i.e., the cross-sex-cross-trait genetic correlations, being of opposite directions. This SA is the main contribution to the asymmetry in **B,** which is again indicative of differences in the multivariate genetic architecture between the sexes. The multivariate SA is driven mostly by testosterone and CBAT as we observed in the cross-trait genetic correlations as well as the cross-sex-cross-cross-trait genetic correlations (r_{mf}^{ct}). Such investigations of SA influenced by testosterone on humans at the genetic level have been lacking, though beneficial role of testosterone in males has been reported (50, 51). In contrast, higher levels of testosterone is known to be harmful in women, increasing the risk of a number of metabolic disorders and cancers (52). This SA at the phenotypic level is also evident from our phenotypic correlations. SA driven by testosterone has been extensively studied in the rodent bank vole, where sexually antagonistic alleles for testosterone have been reported (53). Testosterone also shows intra- and intersexual genetic trade-offs with immune traits in bank voles (54). Remarkably, our results show that testosterone or CBAT is not genetically correlated with fitness in contemporary humans, despite the contributions to antagonism. Hence, in our study, testosterone rather shows hormonal pleiotropy, where it modulates male and female anthropometric traits in opposite directions contributing to the observed SD in these traits.

The r_{mf} for each shared trait between the sexes is extremely high for the anthropometric traits (0.72 to 0.96), almost zero for testosterone. Though we found that testosterone is not genetically correlated with fitness, measures of obesity (BMI, WC, HIP, etc.) are positively correlated with LRS in both the sexes. This suggests that if selection would operate even in one sex, a higher trait value of these anthropometric phenotypes would be favored in both the sexes through the high cross-sex genetic correlation of these traits. For selection on males, this would cause a correlated response of lower testosterone levels in both the sexes, in males through direct cross-trait and in females indirectly through the cross-sex-cross-trait genetic correlations. In contrast for females, a positive selection for these anthropometric traits would lead to high testosterone levels indirectly in males and directly in females through positive cross-sex-cross-trait and cross-trait genetic correlations, respectively. This causes multivariate sexual conflict over the levels of testosterone, and though this would not directly affect fitness due to no significant genetic correlation between testosterone and LRS, it might affect several health parameters. But as we discuss below, these genetic correlations are influenced by the age class of the UKBB participants. Such complexity and intricacies of genetic covariance/correlation strongly emphasize the necessity of using a multivariate framework to study sex difference. Despite the positive correlation between BMI and testosterone in females, we found pleiotropic signals between the two only in males. Moreover, we observed no shared significant variants between the two traits in females, suggesting that testosterone in females is affected by more small-effect loci compared to males, which do not cross the genome-wide significance level.

We observed that the multivariate genetic architecture of the sexes, i.e., $\mathbf{G}_m$ and $\mathbf{G}_f$ are different from each other including and excluding **B**, which is not apparent from studying single traits in isolation. For example, the anthropometric traits are phenotypically dimorphic between the sexes, but the r_{mf} of single traits such as height were extremely high and close to 1, indicating similar genetic architecture between the sexes with no sex-specific difference in genetic variances. This high r_{mf} reflects little or no genetic variation in the traits to be acted on by selection, as dimorphism has already evolved (8). But when we considered the multivariate shared genetic architecture, i.e., **B**, the low, and in certain cases, opposite sign of cross-sex-cross-trait genetic covariances, which are the indirect cross-sex covariances, are suggestive of between-sex differences. This is because these indirect covariances decouples the traits between the sexes and reduces the level of correlated evolutionary response in the sexes when one of them is under selection, hence increasing the level of SD. But irrespective of the contributions of single traits (r_{mf}) to SD, low cross-sex-cross-trait genetic covariances play an important role in the evolution of SD in these traits with otherwise high r_{mf}.

An intriguing result of our study is the role of **B** in the evolution of SD in these traits. **B** constrains the evolution of sexual dimorphism only when selection is sexually antagonistic, by an extreme reduction of the angle of predicted divergence between the sexes, driving them to evolve in more similar directions. In contrast, under concordant selection, **B** neither constrains nor facilitates the evolution of SD. Interestingly, the angle between predicted male and female response after the inclusion of **B** (Fig. 4) is not significantly different between concordant and antagonistic selection. Moreover, we found the r_{mf} of fitness to be significantly less than 1, indicating a partially resolved IASC. This implies that the sexes have not yet reached their sex-specific phenotypic optimum. Our results suggest that sexual dimorphism in these traits is predicted to evolve both under the influence of concordant and antagonistic selection, albeit heavily constrained in the latter case. Sanjak et al. (44) showed that many of the anthropometric traits in humans are under weak sex-specific directional selection, but mostly sexually concordant, except height which is under sexually antagonistic selection. The only study by Stearns et al. that estimated **B** in humans (55), for different phenotypes and pedigree data, also reported the presence of sexually antagonistic selection and a genetic constraint imposed by the **B** matrix.

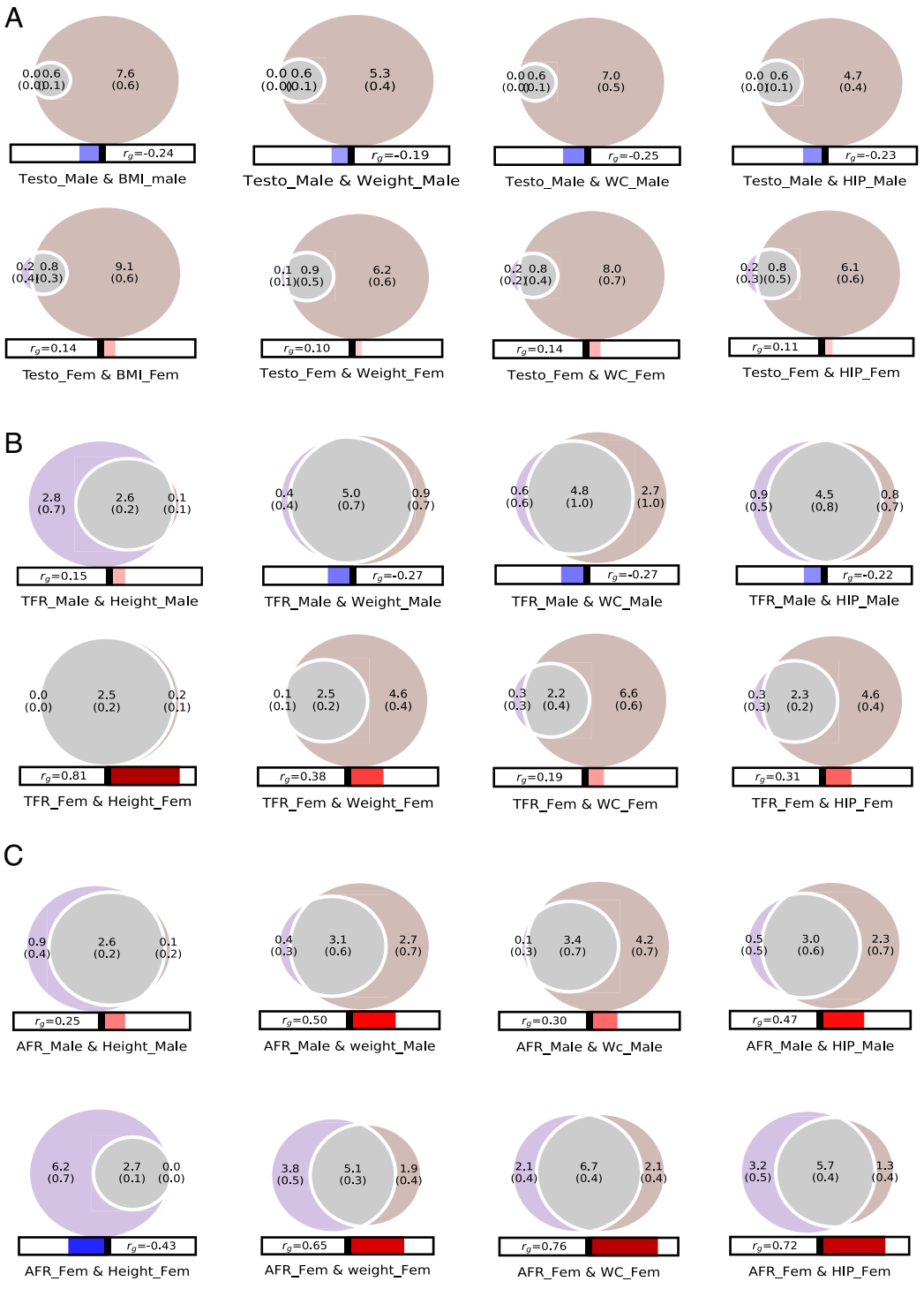

Fig. 4. Venn diagram showing polygenic overlap between testosterone, TFR, AFR, and other anthropometric traits (height, weight, WC, and HIP) in males and females. The number of variants is shown in thousands (with SE). Mauve circles depict unique variants for trait 1, and the brown circle depicts that of trait 2. Shared variants between two traits are shown in gray. r_g depicts the genetic correlation between traits from the MIXeR output. Shades of red denote positive genetic correlations, whereas shades of blue denote negative genetic correlations. Panels represent shared variants between anthropometric traits and (*A*) testosterone, (*B*) TFR, and (*C*) AFR.

An interesting observation in our study is that there is multivariate genetic constraint (46) to evolution in both the male and female genetic architecture, $\mathbf{G}_m$, $\mathbf{G}_f$, as there is no genetic variance in certain directions of the phenotypic space, and with much lower effective dimensionality. But this absence of genetic variance is in different directions in males and females. Such constraints created by the lack of genetic variance in certain directions can result from the presence of negative genetic correlations (46), and we had an abundance of them in our study. Again, these negative genetic correlations in **B** were mostly driven by testosterone and CBAT. In the eigenspace, trunk fat ratio in males and waist circumference in both males and females had higher loadings along these directions of depleted genetic variances. This erosion of genetic variance is very likely the effect of natural/sexual selection on these phenotypes, which resulted in the observed sexual dimorphism in these traits. Hence, there is an absolute genetic constraint along the

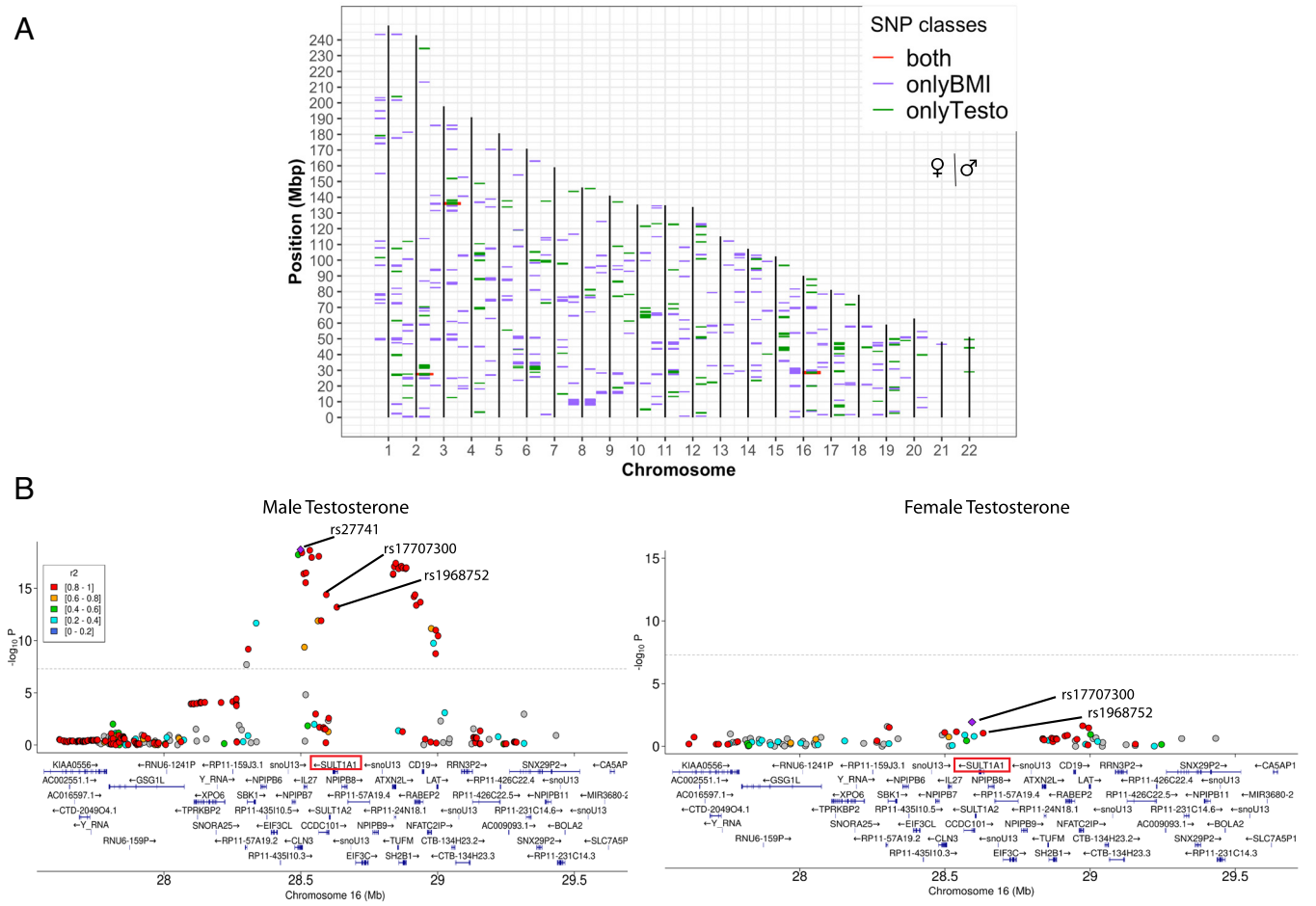

Fig. 5. Genome-wide significant SNPs between testosterone and BMI in males and females. (*A*) Genome-wide SNPs are plotted as colored horizontal lines along chromosomes (*X* axis) at specific positions depicted in mega-base-pairs (*Y* axis), which are significant in 1) both in BMI and testosterone, 2) only in BMI, and 3) only in testosterone. The vertical black lines represent the length of the specific chromosomes. The SNPs to the right of each black line are for males and that to the left of each line are for females. The red horizontal lines show the SNPs that reach the genome-wide significance in both the traits (class 1). (*B*) LocusZoom plots showing variants around the SULT1A1 gene on chromosome 16 for male and female testosterone. The labeled SNPs are 3 of the variants that are identified as shared causal variants on chromosome 16 between testosterone and BMI in males in the colocalization analysis. The same variants are way below the significance threshold for female testosterone. The violet diamond is the lead SNP in the region.

direction of TFR in males and WC in both males and females indicating further selection along those directions would yield no evolutionary response. This study shows the existence of such multivariate absolute genetic constraint in humans, in both the sexes, although for different trait combinations.

The choice of traits also influences the structure and stability of **G** matrices (56). Morphological traits are more stable (i.e., **G** does not change) between populations while fitness estimates are more labile, and physiological traits lie somewhere between these two extremes. The difference in the genetic architecture of the sexes that we observed also depends on the kind of traits that we included in the **G** matrices. In our case, a large proportion of the SA is contributed by testosterone. Previously, SA has been reported for female height and weight with total cholesterol levels in males (55). Similar studies are required to find whether this antagonism prevails across other trait categories in humans.

The age class of UK Biobank participants is between 40 and 69 y (57), and their average age is 56.52 y (58), and hence is biased toward postmenopausal women and older men. Therefore, the antagonistic effect of testosterone can be confounded with age. Nevertheless, our work is still unique in uncovering SA even if limited to a particular age class in humans, as genetic correlations are known to vary with age, both in magnitude and direction (59).

In summary, by investigating the multivariate genetic architecture of three classes of human complex traits we have uncovered considerable sex differences along with a high degree of sexual antagonism which contributes to the observed asymmetry in the shared genetic architecture between sexes (**B**) mostly driven by testosterone. Such antagonism at the genetic level is also reflected at the level of phenotypic correlations. This demands further investigation of SA for other trait categories in humans. Most importantly, we have shown how **B** acts as a constraint to the evolution of sexual dimorphism only when selection is antagonistic. Overall, our work substantially advances the understanding of the biology of male and female multivariate genetic architecture in humans by revealing differences at multiple levels, which would have been otherwise impossible to detect by studying one single trait at a time.

Materials and Methods

GWAS summary statistics for the anthropometric traits except the waist-to-hip ratio (WHR) were downloaded from the Neale lab webpage (http://www.nealelab.is/uk-biobank). Summary statistics for WHR was obtained from the Sulc et al.'s study (https://doi.org/10.1038/s42003-021-02550-y). For the fat depositional and sex-hormonal phenotypes, the GWAS summary statistics were obtained from the studies by Rask-Andersen et al (https://doi.org/10.1038/s41467-018-08000-4) and Sinott-Armstrong et al. (https://doi.org/10.7554/eLife.58615),

respectively. Individual-level data from UK Biobank (https://www.ukbiobank.ac.uk/) accessed with application ID 95478 was only used for calculating phenotypic correlations.

Genetic Covariance and Correlations. We used LDSC regression (43) to estimate all the elements of the $\mathbf{G}_{mf}$ matrix (genetic covariances) as well as the genetic correlations using 12 male and 12 female traits. Three different kinds of genetic correlations were estimated in this study:

a) within-sex, cross-trait genetic correlations:

$$r_{ct} = \frac{\rho_m}{\sqrt{h^2_{im} h^2_{jm}}}, \quad [3]$$

where h^2 is the heritability of traits i and j in males or females, and ρ is the additive genetic covariance between them.

b) cross-sex genetic correlations:

$$r_{mf} = \frac{\rho_{mf}}{\sqrt{h^2_{im} h^2_{if}}}, \quad [4]$$

where ρ_{mf} is the additive genetic covariance between trait i expressed in males and females, and the denominator is the square root of heritabilities of trait i in males and females.

c) cross-sex-cross-trait genetic correlations.

$$r^{ct}_{mf} = \frac{\rho^{ct}_{mf}}{\sqrt{h^2_{im} h^2_{jf}}}, \quad [5]$$

where ρ^{ct}_{mf} is the additive genetic covariance between trait i expressed in males and trait j expressed in females.

All the estimates of genetic correlations were corrected for multiple testing (Benjamini–Hochberg method). Comparison of $\mathbf{G}_m$ and $\mathbf{G}_f$ and the investigation of genetic constraint were done using the random skewers method (48). Asymmetry in **B** was assessed using the *asymmetry* package in R (60). We used MIXeR to estimate polygenic overlap between traits (49). We used the R package *coloc* (61) for detecting colocalized variants between testosterone and BMI, and specifically used *coloc.susie()* (62) to identify multiple shared causal variants. For detailed description of the data analyses, see *SI Appendix*.

Data, Materials, and Software Availability. Previously published data were used for this work [GWAS summary statistics for the anthropometric traits except waist-to-hip ratio (WHR) were downloaded from the Neale lab webpage (https://www.nealelab.is/uk-biobank) (63). Summary statistics for WHR was obtained from the Sulc et al. study (https://doi.org/10.1038/s42003-021-02550-y) (64). For the fat depositional and sex-hormonal phenotypes, the GWAS summary statistics were obtained from the studies by Rask-Andersen et al. (https://doi.org/10.1038/s41467-018-08000-4) (65) and Sinott-Armstrong et al. (https://doi.org/10.7554/eLife.58615) (66), respectively.]. Individual-level data from UK Biobank (https://www.ukbiobank.ac.uk/) (67) accessed with application ID 95478 was only used for calculating phenotypic correlations. Data are available to researchers upon application to the UK Biobank.

ACKNOWLEDGMENTS. We are grateful to Aniket Kumar for helping with the bioinformatic analyses. A.C. is funded by INSPIRE Faculty Fellowship, Department of Science and Technology, Govt. of India, with registration number, IFA20-LSBM-241. D.N. was funded by the National Postdoctoral Fellowship, Science and Engineering Research Board, Govt. of India. We are also thankful to the anonymous reviewers for their insightful comments.

Author affiliations: [a]Biotechnology Research Innovation Council-National Institute of Biomedical Genomics, Kalyani 741251, West Bengal, India; [b]Biostatistics Division, Global Capability Center, GlaxoSmithKline India Global Service Private Limited, Bangalore 560037, India; and [c]School of Arts and Sciences, Azim Premji University, Bengaluru 562125, Karnataka, India

1. E. A. Khramtsova, L. K. Davis, B. E. Stranger, The role of sex in the genomics of human complex traits. *Nat. Rev. Genet.* **20**, 173–190 (2019).
2. E. Bernabeu *et al.*, Sex differences in genetic architecture in the UK Biobank. *Nat. Genet.* **53**, 1283–1289 (2021).
3. K. Rawlik, O. Canela-Xandri, A. Tenesa, Evidence for sex-specific genetic architectures across a spectrum of human complex traits. *Genome Biol.* **17**, 166 (2016).
4. G. A. Blokland *et al.*, Sex-dependent shared and nonshared genetic architecture across mood and psychotic disorders. *Biol. Psychiatry* **91**, 102–117 (2022).
5. C. Ober, D. A. Loisel, Y. Gilad, Sex-specific genetic architecture of human disease. *Nat. Rev. Genet.* **9**, 911–922 (2008).
6. I. Mitra *et al.*, Pleiotropic mechanisms indicated for sex differences in autism. *PLoS Genet.* **12**, e1006425 (2016).
7. R. Lande, Sexual dimorphism, sexual selection, and adaptation in polygenic characters. *Evolution* **34**, 292–305 (1980).
8. R. Bonduriansky, S. F. Chenoweth, Intralocus sexual conflict. *Trends Ecol. Evol.* **24**, 280–288 (2009).
9. J. Poissant, A. J. Wilson, D. W. Coltman, Sex-specific genetic variance and the evolution of sexual dimorphism: A systematic review of cross-sex genetic correlations. *Evolution* **64**, 97–107 (2010).
10. A. Sayadi *et al.*, The genomic footprint of sexual conflict. *Nat. Ecol. Evol.* **3**, 1725–1730 (2019).
11. T. Day, R. Bonduriansky, Intralocus sexual conflict can drive the evolution of genomic imprinting. *Genetics* **167**, 1537–1546 (2004).
12. R. Lande, Quantitative genetic analysis of multivariate evolution, applied to brain: Body size allometry. *Evolution* **33**, 402–416 (1979).
13. T. P. Gosden, S. F. Chenoweth, The evolutionary stability of cross-sex, cross-trait genetic covariances. *Evolution* **68**, 1687–1697 (2014).
14. T. P. Gosden, K.-L. Shastri, P. Innocenti, S. F. Chenoweth, The B-matrix harbors significant and sex-specific constraints on the evolution of multicharacter sexual dimorphism. *Evolution* **66**, 2106–2116 (2012).
15. C. Cheng, D. Houle, Predicting multivariate responses of sexual dimorphism to direct and indirect selection. *Am. Nat.* **196**, 391–405 (2020).
16. F. Ruzicka, L. Holman, T. Connallon, Polygenic signals of sex differences in selection in humans from the UK Biobank. *PLoS Biol.* **20**, e3001768 (2022).
17. J. L. Sztepanacz, D. Houle, Cross-sex genetic covariances limit the evolvability of wing-shape within and among species of *Drosophila*. *Evolution* **73**, 1617–1633 (2019).
18. M. C. Zillikens *et al.*, Sex-specific genetic effects influence variation in body composition. *Diabetologia* **51**, 2233–2241 (2008).
19. J. C. K. Wells, Sexual dimorphism of body composition. *Best Pract. Res. Clin. Endocrinol. Metab.* **21**, 415–430 (2007).
20. I. M. Heid *et al.*, Meta-analysis identifies 13 new loci associated with waist-hip ratio and reveals sexual dimorphism in the genetic basis of fat distribution. *Nat. Genet.* **42**, 949–960 (2010).
21. M. Dieudonne, R. Pecquery, A. Boumediene, M. Leneveu, Y. Giudicelli, Androgen receptors in human preadipocytes and adipocytes: Regional specificities and regulation by sex steroids. *Am. J. Physiol. Cell Physiol.* **274**, C1645–C1652 (1998).
22. T. N. Wittman, C. D. Robinson, J. W. McGlothlin, R. M. Cox, Hormonal pleiotropy structures genetic covariance. *Evol. Lett.* **5**, 397–407 (2021).
23. J. W. McGlothlin, E. D. Ketterson, Hormone-mediated suites as adaptations and evolutionary constraints. *Philos. Trans. R Soc. B, Biol. Sci.* **363**, 1611–1620 (2008).
24. J. C. Randall *et al.*, Sex-stratified genome-wide association studies including 270,000 individuals show sexual dimorphism in genetic loci for anthropometric traits. *PLoS Genet.* **9**, e1003500 (2013).
25. M. Rask-Andersen, T. Karlsson, W. E. Ek, Å. Johansson, Genome-wide association study of body fat distribution identifies adiposity loci and sex-specific genetic effects. *Nat. Commun.* **10**, 339 (2019).
26. K. J. A. Johnston *et al.*, Sex-stratified genome-wide association study of multisite chronic pain in UK Biobank. *PLoS Genet.* **17**, e1009428 (2021).
27. S. E. Graham *et al.*, Sex-specific and pleiotropic effects underlying kidney function identified from GWAS meta-analysis. *Nat. Commun.* **10**, 1847 (2019).
28. H. Choquet *et al.*, A large multiethnic GWAS meta-analysis of cataract identifies new risk loci and sex-specific effects. *Nat. Commun.* **12**, 3595 (2021).
29. L. Dumitrescu *et al.*, Sex differences in the genetic predictors of Alzheimer's pathology. *Brain* **142**, 2581–2589 (2019).
30. C. M. Nievergelt *et al.*, International meta-analysis of PTSD genome-wide association studies identifies sex- and ancestry-specific genetic risk loci. *Nat. Commun.* **10**, 4558 (2019).
31. Y. F. Chiu *et al.*, Sex-specific genetic architecture of human fatness in Chinese: The SAPPHIRe Study. *Hum. Genet.* **128**, 501–513 (2010).
32. J. Martin *et al.*, A genetic investigation of sex bias in the prevalence of attention-deficit/hyperactivity disorder. *Biol. Psychiatry* **83**, 1044–1053 (2018).
33. L. A. Weiss, M. Abney, E. H. Cook, C. Ober, Sex-specific genetic architecture of whole blood serotonin levels. *Am. J. Hum. Genet.* **76**, 33–41 (2005).
34. L. A. Weiss, L. Pan, M. Abney, C. Ober, The sex-specific genetic architecture of quantitative traits in humans. *Nat. Genet.* **38**, 218–222 (2006).
35. G. A. M. Blokland *et al.*, Sex-dependent shared and nonshared genetic architecture across mood and psychotic disorders. *Biol. Psychiatry* **91**, 102–117 (2021), 10.1016/j.biopsych.2021.02.972.
36. E. A. Khramtsova *et al.*, Sex differences in the genetic architecture of obsessive–compulsive disorder. *Am. J. Med. Genet., Part B: Neuropsych. Genet.* **180**, 351–364 (2019).
37. N. Sinnott-Armstrong, S. Naqvi, M. Rivas, J. K. Pritchard, GWAS of three molecular traits highlights core genes and pathways alongside a highly polygenic background. *eLife* **10**, e58615 (2021).
38. K. Watanabe *et al.*, A global overview of pleiotropy and genetic architecture in complex traits. *Nat. Genet.* **51**, 1339–1348 (2019).
39. D. Demontis *et al.*, Genome-wide analyses of ADHD identify 27 risk loci, refine the genetic architecture and implicate several cognitive domains. *Nat. Genet.* **55**, 198–208 (2023).
40. L. M. Kollar *et al.*, The genetic architecture of sexual dimorphism in the moss *Ceratodon purpureus*. *Proc. R. Soc. B* **288**, 20202908 (2021).
41. J. W. McGlothlin, R. M. Cox, E. D. Brodie III, Sex-specific selection and the evolution of between-sex genetic covariance. *J. Hered.* **110**, 422–432 (2019).
42. C. Bycroft *et al.*, The UK Biobank resource with deep phenotyping and genomic data. *Nature* **562**, 203–209 (2018).

43. B. Bulik-Sullivan *et al.*, An atlas of genetic correlations across human diseases and traits. *Nat. Genet.* **47**, 1236–1241 (2015).
44. J. S. Sanjak, J. Sidorenko, M. R. Robinson, K. R. Thornton, P. M. Visscher, Evidence of directional and stabilizing selection in contemporary humans. *Proc. Natl. Acad. Sci. U.S.A.* **115**, 151–156 (2018).
45. T. Connallon, G. Matthews, Cross-sex genetic correlations for fitness and fitness components: Connecting theoretical predictions to empirical patterns. *Evol. Lett.* **3**, 254–262 (2019).
46. B. Walsh, M. W. Blows, Abundant genetic variation + strong selection = multivariate genetic constraints: A geometric view of adaptation. *Annu. Rev. Ecol. Evol. Syst.* **40**, 41–59 (2009).
47. M. W. Blows, A tale of two matrices: Multivariate approaches in evolutionary biology. *J. Evol. Biol.* **20**, 1–8 (2007).
48. J. M. Cheverud, G. Marroig, Comparing covariance matrices: Random skewers method compared to the common principal components model. *Genet. Mol. Biol.* **30**, 461–469 (2007).
49. O. Frei *et al.*, Bivariate causal mixture model quantifies polygenic overlap between complex traits beyond genetic correlation. *Nat. Commun.* **10**, 2417 (2019).
50. D. M. Kelly, T. H. Jones, Testosterone and obesity. *Obes. Rev.* **16**, 581–606 (2015).
51. F. Saad, L. Gooren, The role of testosterone in the metabolic syndrome: A review. *J. Steroid Biochem. Mol. Biol.* **114**, 40–43 (2009).
52. K. S. Ruth *et al.*, Using human genetics to understand the disease impacts of testosterone in men and women. *Nat. Med.* **26**, 252–258 (2020).
53. S. C. Mills, E. Koskela, T. Mappes, Intralocus sexual conflict for fitness: Sexually antagonistic alleles for testosterone. *Proc. R. Soc. B* **279**, 1889–1895 (2012).
54. Eero Schroderus *et al.*, Intra- and intersexual trade-offs between testosterone and immune system: Implications for sexual and sexually antagonistic selection. *Am. Nat.* **176**, E90–E97 (2010).
55. S. C. Stearns, D. R. Govindaraju, D. Ewbank, S. G. Byars, Constraints on the coevolution of contemporary human males and females. *Proc. R. Soc. B* **279**, 4836–4844 (2012).
56. S. J. Arnold, R. Bürger, P. A. Hohenlohe, B. C. Ajie, A. G. Jones, Understanding the evolution and stability of the G-matrix. *Evolution* **62**, 2451–2461 (2008).
57. A. Fry *et al.*, Comparison of sociodemographic and health-related characteristics of UK Biobank participants with those of the general population. *Am. J. Epidemiol.* **186**, 1026–1034 (2017).
58. J. Hewitt, M. Walters, S. Padmanabhan, J. Dawson, Cohort profile of the UK Biobank: Diagnosis and characteristics of cerebrovascular disease. *BMJ Open* **6**, e009161 (2016).
59. S. Stearns, G. de Jong, B. Newman, The effects of phenotypic plasticity on genetic correlations. *Trends Ecol. Evol.* **6**, 122–126 (1991).
60. B. Zielman, asymmetry: Multidimensional scaling of asymmetric proximities (R package version 2.0.4, 2022).
61. C. Giambartolomei *et al.*, Bayesian test for colocalisation between pairs of genetic association studies using summary statistics. *PLoS Genet.* **10**, e1004383 (2014).
62. C. Wallace, A more accurate method for colocalisation analysis allowing for multiple causal variants. *PLoS Genet.* **17**, e1009440 (2021).
63. Neale Lab, GWAS results round 2. https://www.nealelab.is/uk-biobank. Accessed 19 August 2021.
64. J. Sulc *et al.*, "Composite trait Mendelian randomization reveals distinct metabolic and lifestyle consequences of differences in body shape". Zenodo. https://zenodo.org/records/5171807. Deposited 6 August 2021.
65. M. Rask-Andersen *et al.*, Genome-wide association study of body fat distribution identifies adiposity loci and sex-specific genetic effects. *Nat. Commun.* **10**, Article ID 339, (2019).
66. N. Sinnott-Armstrong *et al.*, "GWAS of three molecular traits highlights core genes and pathways alongside a highly polygenic background". Figshare. https://figshare.com/collections/Supplementary_Data_for_Sinnott-Armstrong_and_Naqvi_eLife_2020/5304500/1. Deposited 15 August 2021.
67. C. Bycroft *et al.*, The UK Biobank resource with deep phenotyping and genomic data. UK Biobank. https://www.ukbiobank.ac.uk/. Accessed 5 April 2024.